LBL-24647
UC-210

# Lawrence Berkeley Laboratory
UNIVERSITY OF CALIFORNIA

## APPLIED SCIENCE DIVISION

RECEIVED
LAWRENCE
BERKELEY LABORATORY

APR 1 9 1988

LIBRARY AND
DOCUMENTS SECTION

# Ambient Temperature Secondary Lithium Batteries Using LiAl or Lithium Insertion Anodes

K.M. Abraham

December 1987

TWO-WEEK LOAN COPY

*This is a Library Circulating Copy which may be borrowed for two weeks.*

APPLIED SCIENCE DIVISION

Prepared for the U.S. Department of Energy under Contract DE-AC03-76SF00098

LBL-24647 c.2

## DISCLAIMER

This document was prepared as an account of work sponsored by the United States Government. While this document is believed to contain correct information, neither the United States Government nor any agency thereof, nor the Regents of the University of California, nor any of their employees, makes any warranty, express or implied, or assumes any legal responsibility for the accuracy, completeness, or usefulness of any information, apparatus, product, or process disclosed, or represents that its use would not infringe privately owned rights. Reference herein to any specific commercial product, process, or service by its trade name, trademark, manufacturer, or otherwise, does not necessarily constitute or imply its endorsement, recommendation, or favoring by the United States Government or any agency thereof, or the Regents of the University of California. The views and opinions of authors expressed herein do not necessarily state or reflect those of the United States Government or any agency thereof or the Regents of the University of California.

LBL-24647

# AMBIENT TEMPERATURE SECONDARY LITHIUM BATTERIES USING LiAl OR LITHIUM INSERTION ANODES

Final Report

December 1987

by

**K.M Abraham**

EIC Laboratories, Inc.
111 Downey Street
Norwood, Massachusetts 02062

for

Technology Base Research Project
Lawrence Berkeley Laboratory
University of California
Berkeley, California 94720

This work was supported by the Assistant Secretary for Conservation and Renewable Energy, Office of Energy Storage and Distribution of the U.S. Department of Energy under Contract No. DE-AC03-76SF00098, Subcontract No. 4539410 with the Lawrence Berkeley Laboratory.

ABSTRACT

The feasibility of using $Li_xFe_2O_3$, $Li_xWO_2$ and β-LiAl as alternative anodes for ambient temperature secondary Li batteries was studied. A convenient procedure for the synthesis of these materials at normal temperature and pressure conditions has been developed. The electrochemical behavior of the alternative anode materials was studied in cells utilizing a $TiS_2$ cathode and PC-$LiClO_4$ electrolyte. While the lithiated oxides have exhibited good reversibility, their equivalent weights are too high for use in high energy density batteries. The experimentally determined value for the reversible Li capacity of $Li_xWO_2$ indicated an equivalent weight of 370 for this anode. The corresponding value for $Li_6Fe_2O_3$ was 201. The results obtained with the β-LiAl, synthesized by the new procedure, were too limited to draw meaningful conclusions regarding its usefulness in practical cells.

Amorphous $V_2O_5$, $Cr_3O_8$ and $Li_xCoO_2$ were evaluated as cathodes for possible use in conjunction with the alternative anodes. While the capacities of a-$V_2O_5$ and $Cr_3O_8$, of 2.4 Li/$V_2O_5$ and 4.5 Li/$Cr_3O_8$, respectively, are attractive for practical applications, these positive electrodes exhibited rather low rate capabilities. The performance of $Li_xCoO_2$ was inferior to the results previously reported for the cathode and might have been influenced by the electrolyte employed in our studies.

TABLE OF CONTENTS


| Section | | Page |
|---|---|---|
| | ABSTRACT | i |
| 1.0 | INTRODUCTION | 1 |
| 2.0 | ALTERNATIVE ANODES FOR SECONDARY LITHIUM BATTERIES | 3 |
| | 2.1 Introduction | 3 |
| | 2.2 Experimental | 4 |
| | 2.3 Results and Discussion | 5 |
| | 2.3.1 Synthesis and Characterization of Alternative Anodes | 5 |
| | 2.3.2 Electrochemistry of the Alternative Anodes | 9 |
| | 2.4 Conclusions | 14 |
| 3.0 | HIGH VOLTAGE CATHODES FOR ALTERNATIVE ANODE BATTERIES | 15 |
| | 3.1 Introduction | 15 |
| | 3.2 Experimental | 15 |
| | 3.2.1 Reagents | 15 |
| | 3.2.2 Material Preparation | 16 |
| | 3.2.3 Cell Fabrication | 16 |
| | 3.2.4 Results | 18 |
| | 3.3 Summary | 32 |
| 4.0 | CONCLUSIONS | 33 |
| 5.0 | REFERENCES | 34 |

LIST OF ILLUSTRATIONS


| Figure | | Page |
|---|---|---|
| 1 | X-ray patterns for $Li_xFe_2O_3$ | 7 |
| 2 | X-ray patterns for $Li_xWO_2$ | 8 |
| 3 | Potentiodynamic cycles for $Li_xWO_2/TiS_2$ cells with an *in situ* formed anode. The voltages of the anode versus a $Li^+/Li$ reference electrode are given | 12 |
| 4 | Cell potential (V) vs. capacity (mAh) for $Li_xWO_2/TiS_2$ cell. Current density = 0.5 $mA/cm^2$ | 12 |
| 5 | The first cycle of the cell $Li/Fe_2O_3$ obtained potentiostatically. The voltages of the anode versus a $Li^+/Li$ reference electrode are given | 12 |
| 6 | Potentiodynamic 2nd cycle for $Li_6Fe_2O_3/TiS_2$ cell with an *in situ* formed anode. The voltages of the anode versus a $Li_+/Li$ reference electrode are given | 12 |
| 7 | Cell potential (V) vs. capacity (mAh) for $Li_xFe_2O_3/TiS_2$ cell. Current density = 0.5 $mA/cm^2$ | 12 |
| 8 | FTIR spectra of $V_2O_5$ with and without $P_2O_5$ | 19 |
| 9 | SEM photographs of 90 m/o $V_2O_5$:10 m/o $P_2O_5$ glass before and after sieving | 20 |
| 10 | SEM photographs of 95 m/o $V_2O_5$:5 m/o $P_2O_5$ reaction product | 20 |
| 11 | Potentiodynamic cycling of 90 m/o $V_2$:10 m/o $P_2O_5$ glass vs. Li. Electrolyte was 1.0M $LiClO_4$ in PC | 22 |
| 12 | Room temperature galvanostatic cycling of cell 632-45-16. Cathode composition was 84 w/o $V_2O_5$ (90 m/o:10 m/o):8 w/o Carbon:8 w/o Teflon. Electrolyte was 1.0M $LiClO_4$ in PC | 22 |
| 13a | Room temperature galvanostatic cycling of cell 627-84-17. Cathode composition was 60 w/o $V_2O_5$-$P_2O_5$ (90 m/o:10 m/o):27 w/o Carbon:13 w/o Teflon. Electrolyte was 1.0M $LiClO_4$ in PC | 23 |

13b Room temperature galvanostatic cycling of cell 660-48-29. Cathode composition was 60 w/o $V_2O_5$-$P_2O_5$ (90 m/o:10 m/o):27 w/o Carbon:13 w/o Teflon. Electrolyte was 1.0M $LiClO_4$ in PC. Current density was $\pm$0.5 mA/cm$^2$ for each cycle . . . . . 23

14 Potentiodynamic cycling of cell 627-97-25. Cathode composition was 60 w/o $Cr_3O_8$:27 w/o Carbon:13 w/o Teflon. Theoretical cathode capacity was 135 mAh. . . . 26

15 Galvanostatic cycles for cell 627-97-24. Cathode composition was 60 w/o $Cr_3O_8$:27 w/o Carbon:17 w/o Teflon. Theoretical cathode capacity was 252 mAh. Current density was 0.25 mA/cm$^2$ for discharge and 0.13 for charge. . . . . 26

16 Potentiodynamic cycling of cell 627-68-10. Cathode composition was 84 w/o $LiCoO_2$:8 w/o Carbon:8 w/o Teflon. Theoretical cathode capacity was 168 mAh. . . . 28

17 Galvanostatic cycling curves for cell 627-68-10. Cathode composition was 84 w/o $LiClO_2$:8 w/o Carbon: 8 w/o Teflon. Theoretical cathode capacity was 168 mAh. Current density was $\pm$0.5 mA/cm$^2$. . . . . 30

18 Potentiodynamic cycle for cell 660-50-30. Cathode composition was 60 w/o $LiCoO_2$:27 w/o Carbon:13 w/o Teflon. Theoretical cathode capacity was 49 mAh . . . . 31

19 Galvanostatic cycles for cell 660-50-30. Cathode composition was 60 w/o $LiCoO_2$:27 w/o Carbon:13 w/o Teflon. Current density was 0.25 mA/cm$^2$ . . . . . 31

## LIST OF TABLES

| Table | | Page |
|---|---|---|
| 1 | QUASI-THEORETICAL ENERGY DENSITIES OF SELECTED ALTERNATIVE ANODE BATTERIES. . . . . | 2 |
| 2 | ELECTRONIC CONDUCTIVITY OF INSERTION ANODES. . . . . | 7 |
| 3 | X-RAY DIFFRACTION PATTERN OF β-LiAl. . . . . | 10 |
| 4 | SPECIFICATIONS OF CATHODES USED IN TEST CELLS. . . . . | 17 |

# 1.0 INTRODUCTION

This program is an experimental investigation to assess the practicability of alternative anodes such as LiAl, $LiWO_2$ or $Li_6Fe_2O_3$ for ambient temperature secondary Li batteries. It is hoped that the low Li activity of these electrodes will render them considerably less reactive in organic electrolytes, overcoming the passivation problems and the associated poor cycling efficiency of the Li anode. In addition, the alternative anodes, by virtue of the high solid state diffusion of $Li^+$, may minimize or prevent the tendency to grow dendrites on the anode during cell charging. This is crucial for long cycle life in ambient temperature secondary Li batteries. Cells using the alternative anodes could be significantly safer than Li anode cells, especially in large sizes, because of the low reactivity of the anodes relative to elemental Li.

Alternative anodes have certain limitations: (i) they have higher equivalent weights than Li; (ii) their cells will have lower voltages than those containing Li as the anode. However, these limitations can be mostly overcome by careful selection of the cathodes for use with a given alternative anode. The cathodes of choice for high energy density alternative anode cells are those materials having significantly higher voltages than $TiS_2$, a highly desirable Li insertion cathode for secondary Li batteries. Such materials are known and they include $Cr_3O_8$, $Li_xCoO_2$ and amorphous $V_2O_5$. The synthesis of these cathodes and their electrochemical characterization are some of the tasks in this program.

The aforementioned high voltage cathodes have not so far received significant attention for nonaqueous battery development because of the unavailability of electrolytes suitable for use in the corresponding Li anode

cells. Solvents such as $CH_3CN$, propylene carbonate and sulfolane showing high anodic stability are stable in presence of these cathodes but they do not cycle Li well. However, electrolytes in these solvents can be used with the alternative anodes because of the significantly lower reactivity of the latter electrodes. Energy densities for several alternative anode batteries, estimated on the basis of capacities and voltages taken from literature data, are presented in Table 1.

The results of studies on the alternative anodes $Li_xFe_2O_3$, $Li_xWO_2$ and β-LiAl were presented at the Li Battery Symposium held at the Fall Meeting of the Electrochemical Society in October 1987. The related paper forms Chapter 2 of this report. The data on the oxide cathodes, $Li_xCoO_2$, $Cr_3O_8$ and a-$V_2O_5$ are detailed in Chapter 3.

TABLE 1

QUASI-THEORETICAL ENERGY DENSITIES OF SELECTED ALTERNATIVE ANODE BATTERIES

| Chemical Couple | Mid-Discharge Voltage (V) | Quasi-Theoretical* Specific Energy (Wh/kg) | Quasi-Theoretical* Volumetric Energy Density (Wh/litre) |
|---|---|---|---|
| $Li/TiS_2$ | 2.15 | 480 | 1170 |
| $LiAl/TiS_2$ | 1.75 | 330 | 870 |
| $LiWO_2/TiS_2$ | 1.4 | 112 | 700 |
| $Li_6Fe_2O_3/TiS_2$ | 1.6 | 136 | 570 |
| $LiAl/Li_xCoO_2$ | 3.6 | 759 | 2500 |
| $LiWO_2/Li_xCoO_2$ | 3.2 | 271 | 2560 |
| $Li_6Fe_2O_3/Li_xCoO_2$ | 3.4 | 308 | 1642 |
| $LiAl/Cr_3O_8$ | 2.6 | 641 | 1800 |
| $LiWO_2/Cr_3O_8$ | 2.2 | 198 | 1780 |
| $Li_6Fe_2O_3/Cr_3O_8$ | 2.4 | 355 | 1810 |
| $LiAl/V_2O_5-P_2O_5$ | 2.2 | 688 | 1440 |
| $LiWO_2/V_2O_5-P_2O_5$ | 1.8 | 163 | 1220 |
| $Li_6Fe_2O_3/V_2O_5-P_2O_5$ | 2.0 | 220 | 1310 |

*Does not take into account the mass or volume of associated hardware.

# 2.0 ALTERNATIVE ANODES FOR SECONDARY LITHIUM BATTERIES

## 2.1 Introduction

There have been significant recent advances in the development of ambient temperature secondary Li batteries (1,2). These batteries, comprising the Li anode, organic liquid electrolytes and Li insertion cathodes, have been aimed at applications requiring low to moderate cycle life in the range of 50 to 200 deep discharge cycles. Some potential applications of such systems include power sources for digital communication devices, hand-held tools, electronic equipments and robotics. Secondary Li batteries capable of significantly longer cycle life, e.g., >1000 deep discharge cycles at high energy and power densities, are essential for more demanding applications such as electric vehicle propulsion and load-levelling. Such long cycle life performance is precluded in current ambient temperature secondary Li batteries because of the limited rechargeability of the Li electrode (1,3). The cycle life problems and safety in ambient temperature secondary Li batteries, usually associated with the high reactivity of the elemental Li anode, may be overcome with the use of alternative anodes in which Li activity is less than unity. To this end, $Li_xWO_2$, $Li_xFe_2O_3$ and β-LiAl have been studied. Some of the requirements for alternative anodes, which undergo Li insertion reactions, include:

- A low equivalent weight.
- A small free energy change for the insertion reaction with Li.
- A high diffusivity for $Li^+$ in the solid-state structure of the anode.
- High reversibility for the insertion reaction.
- Good electronic conductivity.

- Thermal stability and chemical compatibility with the electrolyte.
- Ease of fabrication into suitable electrode structures.

Prior work on alternative anodes include the cycling of "rocking chair" cells utilizing in situ formed $Li_xWO_2$ and $Li_xFe_2O_3$ anodes (4,5), and fundamental studies of LiAl electrodes (6,7). Nevertheless, convenient ambient temperature laboratory synthesis procedures are not available for these materials. Such synthetic capability is extremely important for the development of practical batteries with these alternative anodes. Convenient laboratory synthesis at ambient conditions of $Li_xWO_2$, $Li_xFe_2O_3$ and β-LiAl has been developed in this study. Electrochemical behavior of these anodes has been characterized in cells utilizing $TiS_2$ as the cathode. The results are reported.

## 2.2 Experimental

All experiments were carried out in the absence of air and moisture in a Vacuum Atmospheres' Corporation Ar-filled dry box. The α-$Fe_2O_3$ (Johnson-Mathey, 99.999%) and $WO_2$ (Cerac, 99.5%) were dried in vacuo at 190°C and 20 μHg. Al powder (20 microns) was obtained from Aesar Corp. Tetrahydrofuran (THF) was from Burdick and Jackson and it was purified as before (8). Naphthalene (Aldrich 99+%), Li (Foote Mineral Co.), Hexanes (Fisher 99+%) and n-Butyllithium (Alfa) were used as-received. $LiClO_4$ obtained from Alfa Inorganics was dried at 180°C in vacuum. Propylene carbonate (PC), distilled-in-glass, obtained from Burdick and Jackson was dried over 4Å molecular sieves by stirring for about one week at room temperature, and then distilled in vacuum. A one molar solution of $LiClO_4$ in PC was used as the electrolyte.

$TiS_2$ was prepared by a vapor-transport technique (8). All electrodes were made by the pressed powder method from a mixture of the active material with acetylene black carbon and Teflon. The cells were assembled in a manner similar to that employed for the preparation of $Li/TiS_2$ cells (8). Celgard 3401 separator was used in conjunction with PC-containing electrolytes.

X-ray analyses were performed on a Rigaku X-ray diffractor using monochromated $CuK_\alpha$ radiation ($\lambda$ = 1.5405 A).

Electronic conductivities of the electrode materials were measured by the four-point-probe method using pressed pellets.

Cells were cycled using a potentiodynamic (step-potentiostatic) technique, as well as galvanostatically. The potentiostatic technique consists of a computerized potentiostatic sweep over the range of potentials of interest which yields the differential capacity of the cathode as a function of potential. The potential of the cathode is changed by a step value and the current is allowed to decay until it reaches a preset cutoff limit, at which point the next potential step is applied. The corresponding capacity is determined by integrating the current-time curve during the step. The discharge and charge in this manner is performed between preset lower and upper voltage limits. Allowing the cutoff current to decay to a small value, e.g., 50 microamperes, this technique provides rate-independent capacities of the electrodes.

Galvanostatic cycling was performed using standard cycling equipment as described previously (8).

## 2.3 Results and Discussion

### 2.3.1 Synthesis and Characterization of Alternative Anodes

$Li_xWO_2$, $Li_xFe_2$ and β-LiAl were synthesized by a convenient general procedure which involves treatment of the reagents at ambient conditions.

The method involves the reaction of in situ generated Li-naphthalide (Li-naph) with powdered Al or the metal oxides, $Fe_2O_3$ or $WO_2$, in tetrahydrofuran (THF). In this reaction, Li and the anode precursor are taken in stoichiometric amounts, while naphthalene is used in a catalytic amount (9) to solubilize the Li and transport it to the solid metal oxide or Al powder reactant. The presence of only a catalytic amount of naphthalene prevents complications resulting from side reactions of Li-naph with THF. In a typical preparation of $Li_xFe_2O_3$, 0.5g (~4 mmoles) of naphthalene was used in a reaction with ~5g (~31 mmoles) of the oxide in 50 ml of THF. Lithium was taken in amounts equivalent to the required value of x in $Li_xFe_2O_3$. The mixture was stirred intermittently over a one-week period. At the end of this time, the solid was filtered and washed with excess THF. The filtrate was hydrolyzed with water and titrated with standard HCl to determine the amount of unreacted Li-naphthalide and consequently, the stoichiometry of the lithiated product. $Li_xFe_2O_3$ where x = 1, 2, 3, 4, 5 and 6 were synthesized. X-ray analysis revealed that lithiation results in a loss of crystallinity of the oxide with the highly lithiated materials becoming amorphous. This is depicted in Figure 1. The x-ray data appears to show that $Li_xFe_2O_3$, where $1<x\leq3$, are poorly crystalline materials; while, $Li_xFe_2O_3$ were $3<x\leq6$, are amorphous. Lithiation also brought about changes in the conductivity of the iron oxide, Table 2. Thus, although $\alpha$-$Fe_2O_3$ is an insulator, all of the lithiated materials were found to have good conductivity with values of 0.44 $(ohm\text{-}cm)^{-1}$ for $Li_3Fe_2O_3$ and 0.40 $(ohm\text{-}cm)^{-1}$ for $Li_6Fe_2O_3$. This is practically significant since it would be possible to fabricate useful $Li_6Fe_2O_3$ anodes without incorporating carbon in the electrodes for conductivity enhancement. Both $\alpha$-$Fe_2O_3$ and

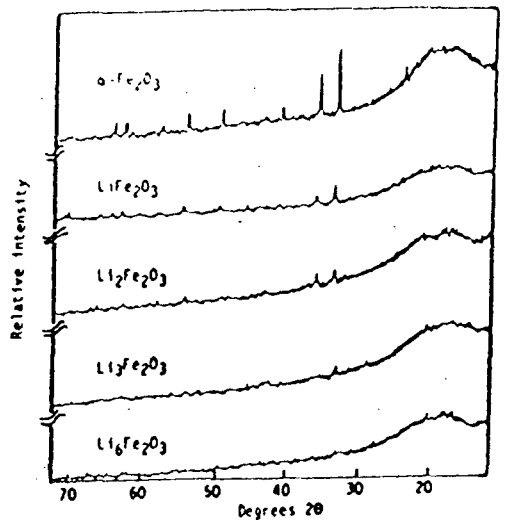


Fig. 1. X-ray patterns for $Li_xFe_2O_3$.

TABLE 2

ELECTRONIC CONDUCTIVITY OF INSERTION ANODES

| Compound | Pressure Used for Pellet Preparation (psi x $10^6$) | Conductivity $(\Omega\text{-cm})^{-1}$ |
|---|---|---|
| $\alpha$-$Fe_2O_3$ | 1.1 | $10^{-13}$ |
| $LiFe_2O_3$ | 1.1 | $5.3 \times 10^{-2}$ |
| $Li_2Fe_2O_3$ | 1.1 | $3.0 \times 10^{-1}$ |
| $Li_3Fe_2O_3$ | 1.1 | $4.4 \times 10^{-1}$ |
| $Li_4Fe_2O_3$ | 1.1 | $3.4 \times 10^{-1}$ |
| $Li_5Fe_2O_3$ | 1.1 | $2.5 \times 10^{-1}$ |
| $Li_6Fe_2O_3$ | 1.1 | $4.0 \times 10^{-1}$ |
| $WO_2$ | 2.5 | 55 |
| $Li_{0.5}WO_2$ | 2.5 | 4.4 |
| $Li_{1.0}WO_2$ | 2.5 | 1.9 |
| LiAl | 2.5 | $1.43 \times 10^3$ |

$\gamma$-$F_2O_3$ behaved identically. The conductivity of $\gamma$-$F_2O_3$ is $3x10^{-5}$ $(ohm\text{-}cm)^{-1}$ and rises to $3x10^{-2}$ $(ohm\text{-}cm)^{-1}$ in $\gamma$-$Li_6Fe_2O_3$. A loss of crystallinity was observed upon lithiation of this form of $Fe_2O_3$ as well.

Starting with $WO_2$, $Li_{0.5}WO_2$ and $Li_{1.0}WO_2$ have been synthesized. The X-ray diffraction patterns of these materials are presented in Figure 2. As the Li content is increased, the diffraction peaks become broader, and the principal peak at 3.44A is greatly reduced in intensity in $Li_{1.0}WO_2$. These features may indicate crystallite size reduction or perturbations of the lattice as a result of Li insertion. The fact that the basic X-ray pattern remains the same even after an uptake of 1 Li per mole of $WO_2$ strongly supports an insertion process for the Li reaction. Both of the lithiated products are electronic conductors. The measured conductivities are: $WO_2$, 55 $(ohm\text{-}cm)^{-1}$; $Li_{0.5}WO_2$, 4.4 $(ohm\text{-}cm)^{-1}$ and $Li_{1.0}WO_2$, 1.9 $(ohm\text{-}cm)^{-1}$. Again, these conductivities are adequate to allow these materials to function as electrodes without the use of a conductivity enhancing additive such as carbon.

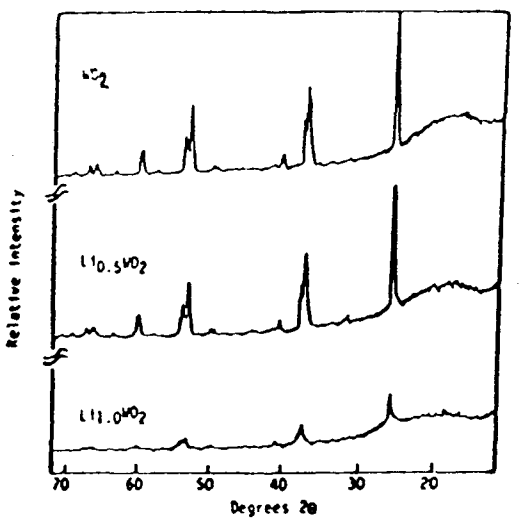


Fig. 2. X-ray patterns for $Li_xWO_2$.

Attempts were made to prepare $Li_xFe_2O_3$ and $Li_xWO_2$ from reactions of the respective oxide with n-butyllithium in hexane (10). Even in reactions involving a large excess of n-butyllithium, a maximum of only ~0.2 mole of Li per mole of $WO_2$ could be incorporated into $WO_2$, and only ~0.7 mole of Li per mole of $\alpha$-$Fe_2O_3$ could be incorporated into the iron oxide. It appears that n-BuLi, with an oxidation potential approximately 0.5V more positive than that of Li-naph, is not capable of driving the lithiation of the oxides to completion. The Li-naphthalide reaction, with the modification described in this paper, appears to be a more general technique for the preparation of Li insertion electrodes, irrespective of their reduction potentials.

The reaction of Al powder (20 micron size) with a stoichiometric amount of Li, in presence of a small amount of naphthalene in THF, can go to completion at room temperature. Preparation of an alloy with the nominal stoichiometry of $Li_{0.98}Al$ was achieved. The product is a free-flowing powder, and the Debye-Scherrer X-ray pattern of this material (Table 3) shows the six principal Bragg lines for $\beta$-LiAl, along with a trace of unreacted Al. The reaction of Li-naphthalide with Al powder, however, was slow at room temperature requiring 2 to 3 weeks for completion. The rate of this reaction can probably be improved by removing the oxide surface coating of the aluminum powder. The conductivity of the $\beta$-LiAl thus prepared was determined to be $1.4 \times 10^3$ $(ohm\text{-}cm)^{-1}$.

2.3.2 Electrochemistry of the Alternative Anodes

The electrochemical behavior of the anodes, particularly their reversibility, was investigated in cells of the configuration,

alternative anode/PC-$LiClO_4$/$TiS_2$

where the alternative anode is $Li_{1.0}WO_2$, $Li_6Fe_2O_3$ or $\beta$-LiAl. The anodes formed in two different ways were investigated. In the first series of

TABLE 3

X-RAY DIFFRACTION PATTERN OF β-LiAl

| D, Å | $I/I_0$ | D, Å | $I/I_0$ |
|---|---|---|---|
| 3.63 | 100 | 3.65 | 100 |
| 2.35* | 5 | | |
| 2.23 | 100 | 2.26 | 100 |
| 2.03* | 10 | | |
| 1.91 | 80 | 1.92 | 75 |
| 1.58 | 50 | 1.58 | 60 |
| 1.46 | 50 | 1.46 | 60 |
| 1.29 | 70 | 1.30 | 100 |
| 1.22 | 40 | 1.22 | 75 |

*Unreacted Al.

cells, to study the behavior of pristine materials, the anodes were formed in situ. In this configuration, a Li electrode is also inserted into the cell and it is placed, with appropriate electronic insulation, next to an electrode of the anode precursor, i.e., $WO_2$, $Fe_2O_3$ or Al. The initial discharge is performed between the Li electrode and the anode precursor. Beginning with the second cycle, Li is cycled between $TiS_2$ and the in situ formed alternative anode. In the second type of cells the alternative anode is fabricated with materials synthesized as described earlier. In cycle testing, the initial few cycles of a cell were obtained potentiodynamically to assess the rate independent capacity of the anode. This was followed by extensive galvanostatic cycling.

**$Li_1WO_2$:** The first three potentiodynamically obtained cycles of a $Li_xWO_2$/PC-$LiClO_4$/$TiS_2$ cell with in situ formed $Li_xWO_2$ anode are given in Figure 3. A capacity of approximately 0.8 $Li/WO_2$, based on a theoretical utilization of 1 Li per mole of the oxide was obtained in all three cycles. Two inflection points at ~1.7V and ~0.8V (given as the voltage of the anode

versus a Li reference) are seen in both the discharge (oxidation of $Li_xWO_2$) and the charge (reduction of $WO_2$) half-cycles of the cell. The lower inflection point may be associated with a phase change of $WO_2$ as Li inserted into it (11). The small amount of capacity beyond the upper inflection point at 1.7V may be due to the discharge and charge of a small amount of $WO_3$ present as an impurity in $WO_2$. Some reduction of the PC electrolyte may occur at ~0.6V as there is a slightly higher reduction capacity for the anode in each charge half-cycle than its capacity in the preceding oxidation. Subsequent to the potentiostatic cycles of Figure 3, the cell was cycled galvanostatically between the voltage limits of 0.5 and 2.2V. The current density was 0.5 $mA/cm^2$. Figure 4 shows typical cycles. More than one hundred cycles were obtained. The $WO_2$ utilization was ~0.5 equivalents of Li in the fifth cycle and ~0.4 $Li/WO_2$ after 113 cycles. The rechargeability of the $Li_xWO_2$ electrode appears to be extremely good, although its specific utilization is only modest.

**$Li_6Fe_2O_3$:** Typical cycles of a $Li_6Fe_2O_3$/PC-$LiClO_4$/$TiS_2$ cell with an <u>in situ</u> formed $Li_6Fe_2O_3$ anode are given in Figures 5 and 6. The reduction of $Fe_2O_3$ initially takes place within a relatively narrow potential region and two clearly discernible inflection points are seen in the voltage-capacity curve. These may correspond to phase transitions in $Li_xFe_2O_3$ for values of x=2 and x=5. The oxidation of $Li_xFe_2O_3$ (i.e., discharge of the $Li_xFe_2O_3/TiS_2$ cell) is accompanied by a large swing in voltage of the anode (compared with the reduction potential) with a mid-oxidation potential of ~1.7V. Of the six Li inserted into the $Fe_2O_3$ in the first reduction, only about three could be extracted out in the oxidation. This three Li capacity as shown in Figure 6 could be cycled with nearly 100% efficiency in the following potentiodynamic cycles. Typical galvanostatic cycles of the $Li_6Fe_2O_3/TiS_2$ cell, between

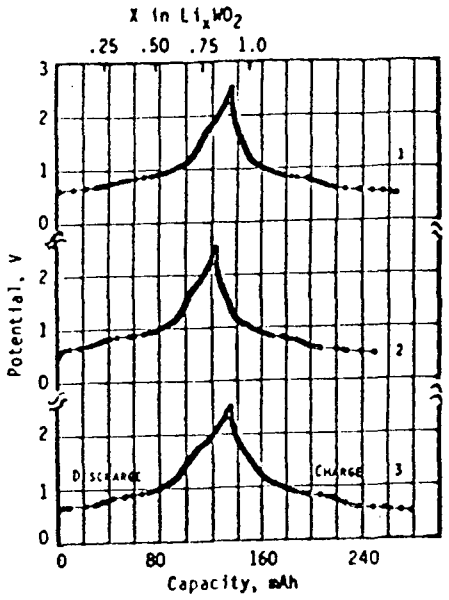


Fig. 3. Potentiodynamic cycles for $Li_xWO_2/TiS_2$ cell with an in situ formed anode. The voltages of the anode versus a $Li^+/Li$ reference electrode are given.

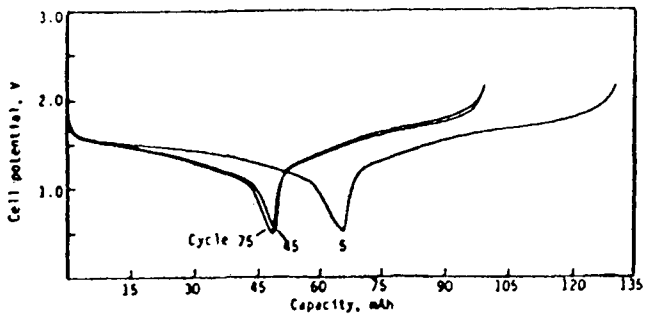


Fig. 4. Cell potential (V) vs. capacity (mAh) for $Li_xWO_2/TiS_2$ cell. Current density = 0.5 $mA/cm^2$.

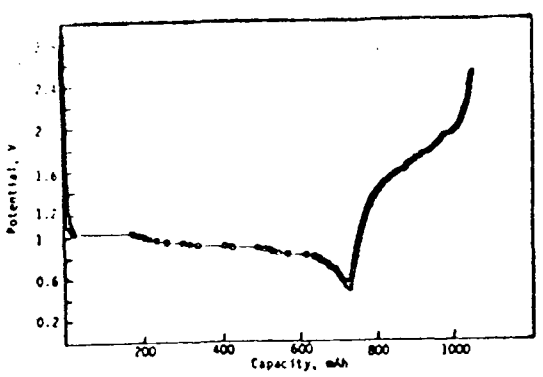


Fig. 5. The first cycle of the cell $Li/Fe_2O_3$ obtained potentiostatically. The voltages of the anode versus a $Li^+/Li$ reference electrode are given.

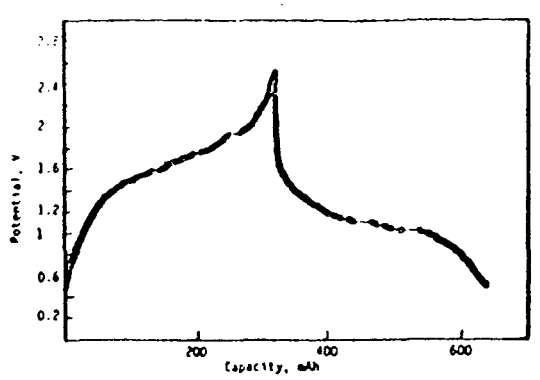


Fig. 6. Potentiodynamic 2nd cycle for $Li_6Fe_2O_3/TiS_2$ cell with an in situ formed anode. The voltages of the anode versus a $Li^+/Li$ reference electrode are given.

2.2 and 0.5V at 0.5 mA/cm$^2$, obtained subsequent to the cycles in Figures 5 and 6, are shown in Figure 7. More than 100 cycles were obtained and the $Li_xFe_2O_3$ utilization decreased from 0.9 Li/$Li_6Fe_2O_3$ in the fifth cycle to ~0.4 Li after 113 cycles.

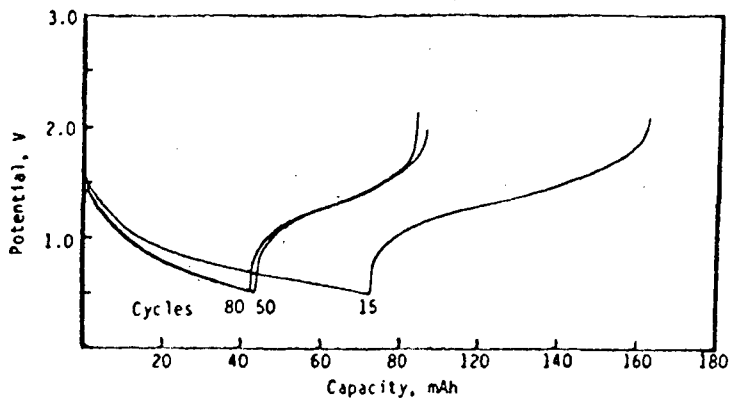


Fig. 7. Cell potential (V) vs. capacity (mAh) for $Li_xFe_2O_3/TiS_2$ cell. Current density = 0.5 mA/cm$^2$.

By incrementally inserting Li into $\alpha$-$Fe_2O_3$ under controlled current conditions and extracting the Li out by a potentiodynamic charge to 2.5V we have confirmed that the first three Li inserted into $\alpha$-$Fe_2O_3$ are irreversible. The last three Li incorporated are the reversible ones. The cycling results indicate that a major drawback of the $Li_6Fe_2O_3$ anode is the large voltage swing to higher potentials following Li insertion in the first reduction of $Fe_2O_3$. As a result only about one Li can be cycled within a practically useful voltage range. With a useful capacity of only about one Li per $Li_6Fe_2O_3$, the equivalent weight of this anode is a rather high 201.

The $Li_6Fe_2O_3$ anode, chemically prepared as described earlier, was cycled in the same manner as the <u>in situ</u> prepared electrode. The initial discharge capacity of a $Li_6Fe_2O_3/TiS_2$ cell cycled between 2.2 and 0.5V at 0.5 mA/cm$^2$ was equivalent to 0.9 Li. The recharge efficiency was 100%. However,

the capacity faded somewhat rapidly with cycling. One reason for this may have been the absence of any carbon in the electrode.

**β-LiAl Anode:** Preliminary electrochemical investigations were performed with β-LiAl prepared by the Li-naph method. An electrode was prepared by pressing the β-LiAl powder with a small amount of Teflon, and a cell of the configuration β-LiAl/PC-$LiClO_4$/$TiS_2$ was constructed. It exhibited an open circuit potential of 1.72V. Measurement of the β-LiAl voltage against a Li reference electrode showed a voltage of 0.38V. These values are consistent with a β-LiAl anode cell. Upon discharging the cell at 0.1 $mA/cm^2$, a substantial polarization of the anode occurred after delivering a capacity of ∿10 mAh, which is only ∿3% of the theoretical Li capacity. It appeared that β-LiAl powder electrode had very low rate capability. Improved techniques to prepare pressed electrodes with β-LiAl powder appear to be necessary in order to fully assess its electrochemical behavior.

## 2.4 Conclusions

A convenient procedure for the synthesis of alternative anodes such as $Li_xFe_2O_3$, $Li_xWO_3$ and β-LiAl has been developed. The electrochemical behavior of $Li_xFe_2O_3$ and $Li_xWO_3$ has been evaluated. The experimental results indicated a practical equivalent weight of ∿201 for the $Li_xFe_2O_3$ anode, and ∿370 for the $Li_xWO_2$ anode.

# 3.0 HIGH VOLTAGE CATHODES FOR ALTERNATIVE ANODE BATTERIES

## 3.1 Introduction

The proper choice of the cathode candidate is extremely important in achieving practical success with the alternative anode battery concept. Some of the desirable properties of insertion cathodes for these types of batteries are:

- High discharge potentials versus $Li^+/Li$,
- low equivalent weight,
- high solid-state diffusion for $Li^+$,
- chemical compatibility with the electrolyte.

Three transition metal oxides have been evaluated in this program. They are amorphous $V_2O_5$, $Cr_3O_8$, and $Li_xCoO_2$. These materials have been previously studied in relation to their use in Li anode batteries (12-14). However, an assessment of their utility in alternative anode batteries is being carried out for the first time.

## 3.2 Experimental

### 3.2.1 Reagents

$V_2O_5$ (99.995%), $P_2O_5$ (99.998%), $CrO_3$ (99.998%), and $Li_2CO_3$ (99.999%) were obtained from Johnson Matthey and used as-received. Tetrahydrofuran was from Burdick and Jackson, and was purified as before (8). Lithium metal (Foote Mineral Co.), Naphthalene (Aldrich 99+%). Hexanes (Fisher 99+%), and n-Butyllithium (Alfa) were also used as-received. Propylene Carbonate (PC), distilled-in-glass (Burdick and Jackson) was dried over 4A molecular sieves by stirring for about one week at room temperature, and then distilled in vacuum. $LiClO_4$ obtained from Alfa Inorganics was dried at 180°C in vacuum. The electrolyte was 1.0M $LiClO_4$ in PC. The separator used in the test cells was Celgard™ 3401.

### 3.2.2 Material Preparation

**$V_2O_5$-$P_2O_5$ Glass:** This material was prepared in two compositions; 90 mole-percent (m/o) $V_2O_5$:10 m/o $P_2O_5$ and 95 m/o $V_2O_5$:5 m/o $P_2O_5$. The powdered oxides were mixed under Argon in a 2 liter round bottom flask with a magnetic stirring bar for 5 h. The natural tumbling action of the material which crept up the flask wall was augmented by periodically removing the flask from the stirrer and shaking it manually. The $V_2O_5$ glass was prepared by slowly heating one of these mixtures to 750°C in a silica crucible, maintaining this temperature for 1 hr, and then quenching the melt in an ice-water bath.

**$Cr_3O_8$:** Twenty-five grams of $CrO_3$, dried overnight at 150°C, were ground under Argon in an agate mortar, and transferred to a silica boat. The ground powder was heated in air at 280°C for 21 hours, then transferred to a dry box.

**$LiCoO_2$:** The appropriate stoichiometric amounts of $Li_2CO_3$ and $CoCO_3$ were mixed by the technique described above for the Vanadium glass. The mixture was pelletized and heated in air at 900°C for 20 hours.

All three of these materials were ground under Ar in an agate mortar; best results for cathode fabrication were obtained with samples that were passed through a 200 mesh sieve prior to use.

X-ray analyses, electronic conductivities, and cell cycling experiments were performed as described in Chapter 2. Samples of the vanadium glasses were also examined by Scanning Electron Microscopy (SEM) and Fourier Transform Infrared Spectroscopy (FTIR).

### 3.2.3 Cell Fabrication

In most cases, the cells consisted of pressed cathodes sandwiched between two Li electrodes. Cathodes were prepared as pressed powder electrodes for which intimate mixtures of the appropriate cathode material with sintered

Carbon/Teflon mixtures were pressed onto one side of expanded Ni screens (Exmet Corporation, 3-Ni-3.3) at 9000 psi. The cathode area was 10 $cm^2$ in each case. Cathode loading capacities and thicknesses varied, and are given in Table 4. Each Li electrode had an area of 10 $cm^2$/side; the one facing the back of the cathode served as a reference electrode. The anodes were fabricated by pressing 10 mil Li foil strips onto both sides of a Ni screen. A large excess of Li was used, and all electrodes were bagged in two layers of Celgard™ 3401 polypropylene separator. The electrode package was placed in a D-cell can (Ni-plated, cold-rolled steel) and compression was applied to the electrode package by Teflon hemicylinders and stainless steel shims. The cover assembly was fitted to the can via an O-ring seal, and the cell was vacuum filled with electrolyte through a tube on the cell cover. Electrical connections to the electrode package were made through a Conax™ fitting on the cover.

TABLE 4

SPECIFICATIONS OF CATHODES USED IN TEST CELLS

| Cell No. | Material | Composition* | Theoretical Capacity (mAh) | Weight of Mixture (g) | Thickness (cm) |
|---|---|---|---|---|---|
| 627-84-17 | 90 m/o $V_2O_5$<br>10 m/o $P_2O_5$ | 60:27:13 | 254 | 0.96 | 0.091 |
| 632-45-16 | 90 m/o $V_2O_5$<br>10 m/o $P_2O_5$ | 84:8:8 | 375 | 0.99 | 0.075 |
| 660-48-29 | 90 m/o $V_2O_5$<br>10 m/o $P_2O_5$ | 60:27:13 | 76 | 0.28 | 0.033 |
| 627-97-24 | $Cr_3O_8$ | 60:27:13 | 252 | 0.99 | 0.074 |
| 627-97-25 | $Cr_3O_8$ | 60:27:13 | 135 | 0.53 | 0.048 |
| 627-68-10 | $LiCoO_2$ | 84:8:8 | 168 | 0.61 | 0.061 |
| 627-50-30 | $LiCoO_2$ | 60:27:13 | 49 | 0.30 | 0.046 |

*Weight ratio of cathode material, carbon and Teflon.

### 3.2.4 Results

**$V_2O_5$-$P_2O_5$ Glass:** Glassy $V_2O_5$ was prepared from both a 90 m/o $V_2O_5$:10 m/o $P_2O_5$ and a 95 m/o $V_2O_5$:5 m/o $P_2O_5$ mixture, respectively. Debye-Scherrer X-ray photographs indicated that the product obtained from the mixture containing 10 m/o $P_2O_5$ was amorphous (i.e., without long-range crystalline order), whereas two aliquots of a 95 m/o $V_2O_5$:5 m/o $P_2O_5$ mixture subjected to the same heat treatment displayed the X-ray diffraction pattern of crystalline $V_2O_5$. Figure 8 is a composite showing the FTIR spectra of the $V_2O_5$ reagent used, the 95% m/o $V_2O_5$ 'glass', and 90 m/o $V_2O_5$ glass. As reported previously (12), the introduction of $P_2O_5$ into $V_2O_5$ results in a broadening of the IR spectra, indicative of variations in V-O bond lengths. With our samples, however, this behavior was only observed when 10 m/o $P_2O_5$ was used. The glassy material had a conductivity of $1.98 \times 10^{-5}$ $(ohm\text{-}cm)^{-1}$ and SEM photographs showed a wide range of irregular particle shapes and sizes even when the ground materials were passed through a 200 mesh sieve. Particle dimensions ranged from 0.3 to 400 microns. Figure 9 is a comparison of the glass containing 10 m/o $P_2O_5$ before and after sieving. Figure 10 is a similar comparison for the material with 5 m/o $P_2O_5$. The magnification is 500X in all cases. Although the range of particle sizes appears to be the same, the distribution appears to be different. The crystalline sample, containing only 5 m/o $P_2O_5$ appears to have a greater proportion of small particles. This coincides with the fact that it was easier to grind. When the 10 m/o $P_2O_5$ glassy samples was contacted with an excess of n-butyllithium, the maximum uptake of Li was 3 Li/$V_2O_5$. By comparison, the crystalline sample with 5 m/o $P_2O_5$ had an uptake ratio of 6 Li/$V_2O_5$ with subsequent X-ray analysis showing that it had undergone such an extensive reduction that it resembled a vanadium oxide of approximate stoichiometry VO.

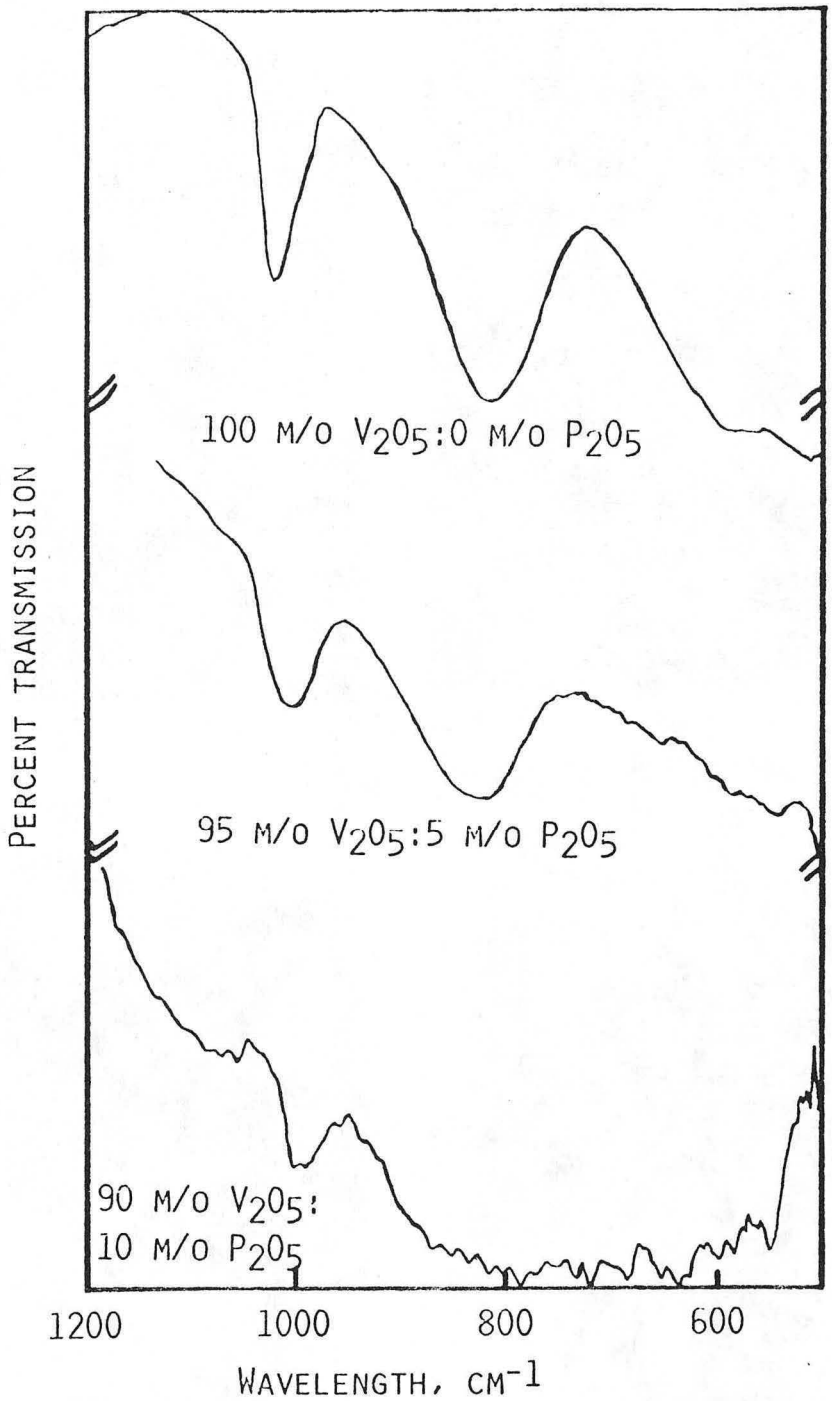


Fig. 8. FTIR spectra of $V_2O_5$ with and without $P_2O_5$.

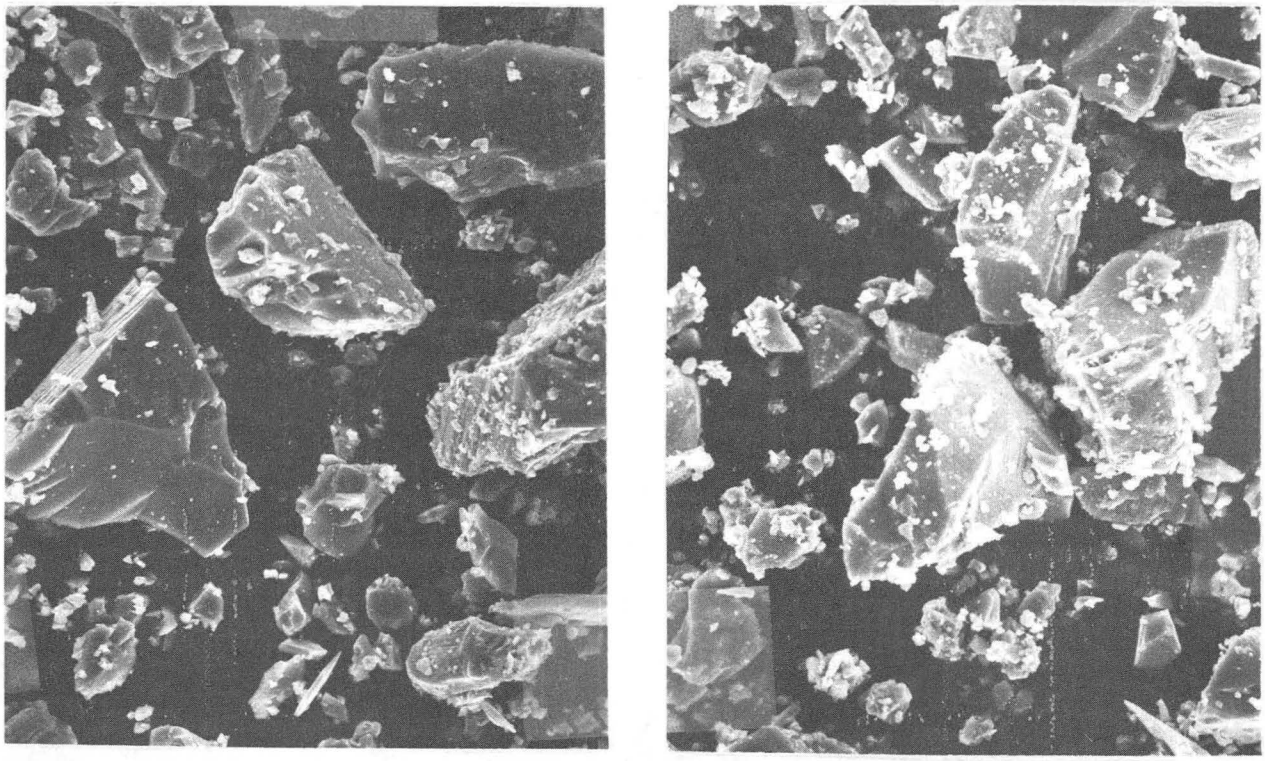

Unmeshed Passed through 200 mesh

Fig. 9. SEM photographs of 90 m/o $V_2O_5$:10 m/o $P_2O_5$ glass before and after sieving. Magnification 500X.

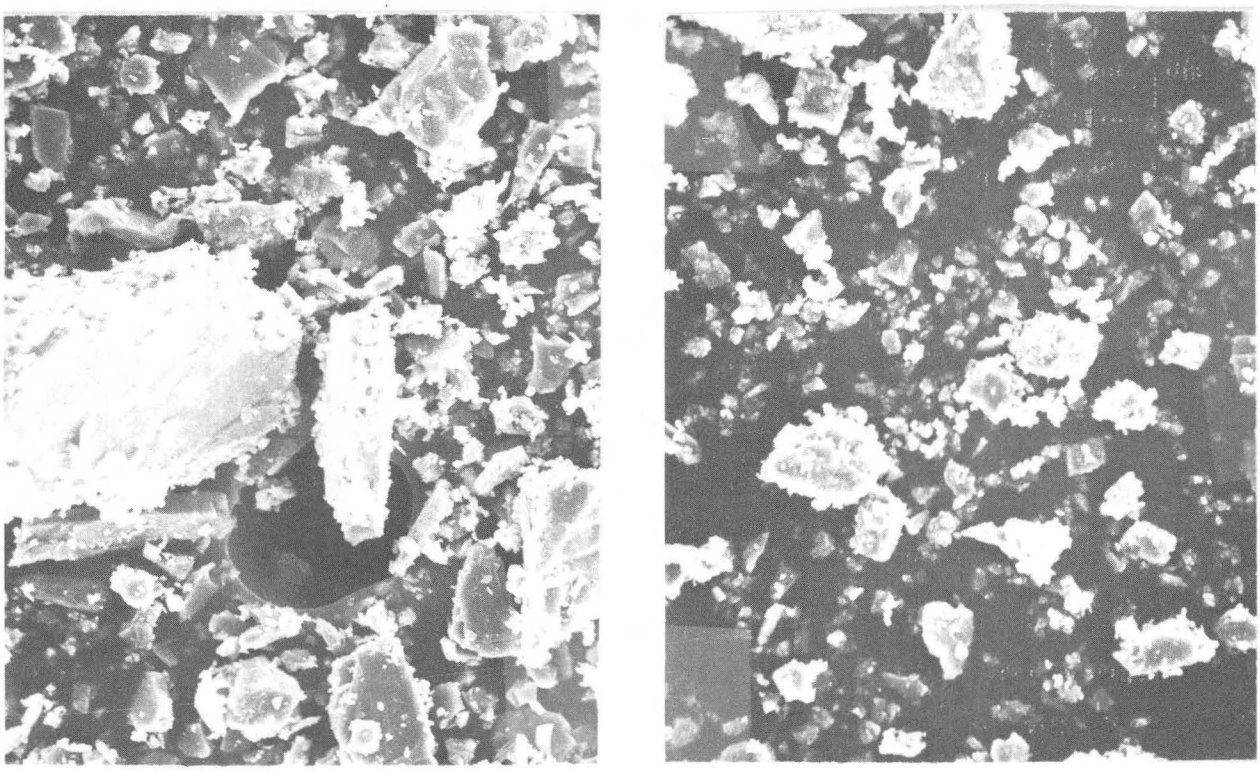

Unmeshed Passed through 200 mesh

Fig. 10. SEM photographs of 95 m/o $V_2O_5$:5 m/o $P_2O_5$ reaction product. Magnification 400X.

Figure 11 is a cycling curve (cathode potential vs. cumulative capacity) under rate independent (i.e., potential controlled) conditions for cell 632-45-16. The cathode composition was 84 w/o $V_2O_5$-$P_2O_5$ (90 m/o:10 m/o):8 w/o Carbon:8 w/o Teflon, and the cell configuration was Li/PC-$LiClO_4$/cathode. When this cell was discharged from the open circuit voltage (OCV) of 3.6V to 1.5V vs. $Li^+$/Li, the observed capacity was 269.6 mAh, corresponding to a utilization of 2.4 Li/$V_2O_5$. When the cell was recharged to a limit of 4.0V, a capacity of 182 mAh was observed, corresponding to 67.6% of the discharge capacity. Three voltage plateaus are evident in the discharge curve at 2.1, 1.8, and 1.6V vs. $Li^+$/Li. There is a large voltage swing during the recharge. The comparison of the capacities of the two half cycles indicates that 22% of the observed discharge capacity is irreversible. When this cell was cycled at room temperature under galvanostatic conditions, it was observed that the maximum capacity could be obtained at a current density of 0.25 mA/$cm^2$. Figure 12 shows that repeated galvanostatic cycling between 4.0 and 1.5V at this rate caused the discharge capacity to improve with cycling. The discharge capacity increased from 151.8 mAh (1.35 Li/$V_2O_5$) in the first galvanostatic cycle to 190 mAh (1.68 Li/$V_2O_5$) for the eleventh cycle. When the current density was doubled for the twelfth cycle the capacity decreased to 150 mAh, then diminished rapidly so that by cycle 14 it was 58 mAh (0.91 Li/$V_2O_5$), with virtually no recharge occurring below 2.5V.

Figure 13 is a composite showing the results of galvanostatic cycling for two cells with the same configuration as the one described above, but with a cathode composition of 60 w/o $V_2O_5$-$P_2O_5$ (90 m/o $V_2O_5$:10 m/o $P_2O_5$):27 w/o Carbon:13 w/o Teflon. The cathode material in cell 660-48-29 had been passed through a 200 mesh sieve, while the material in cell 627-84-17 was not. One would expect that the sieved material, having a more uniform dis-

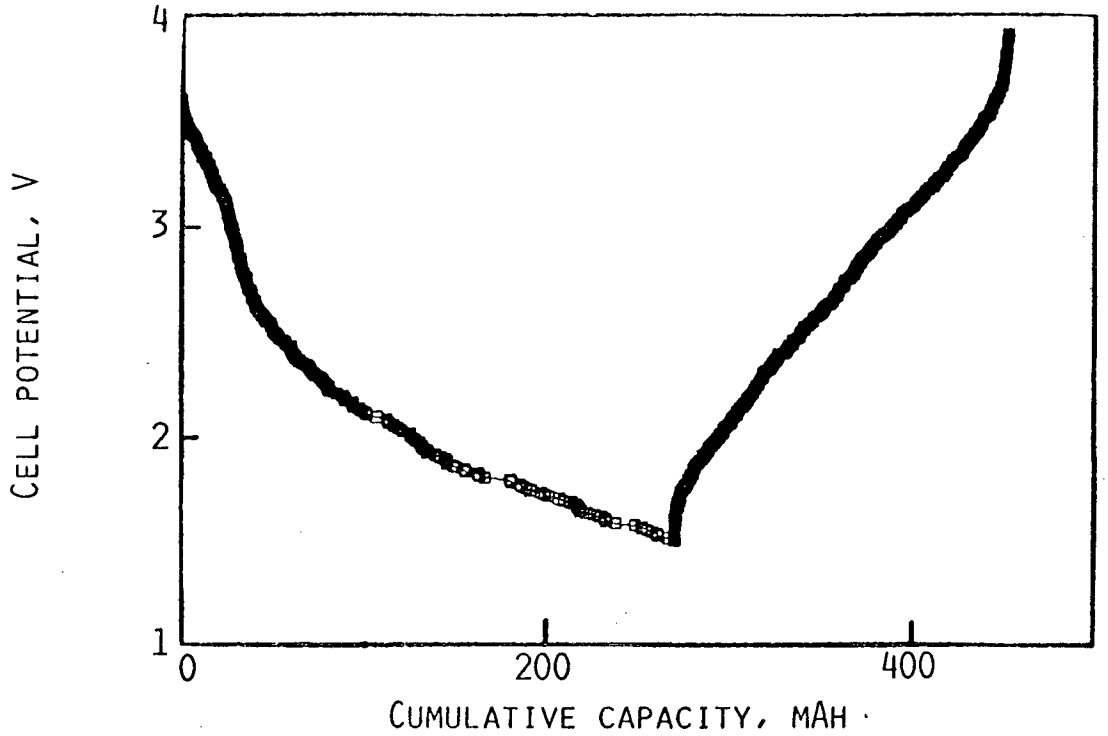


Fig. 11. Potentiodynamic cycling of 90 m/o $V_2O_5$:10 m/o $P_2O_5$ glass vs. Li. Electrolyte was 1.0M $LiClO_4$ in PC.

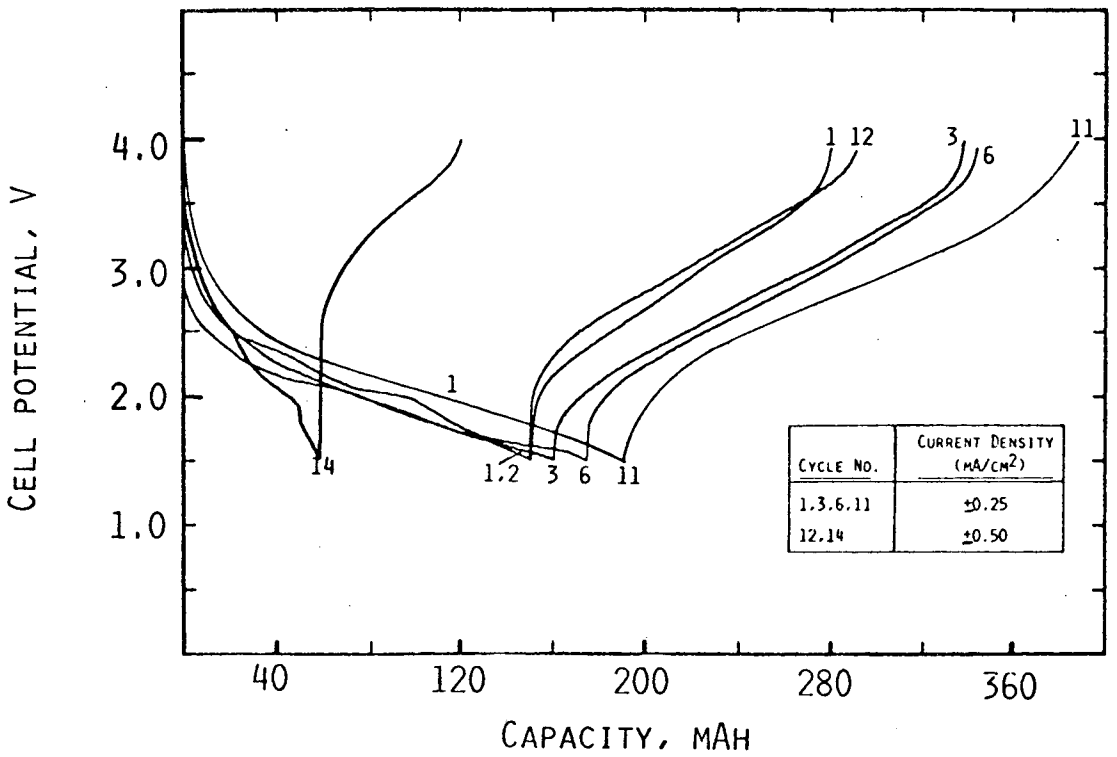


Fig. 12. Room temperature galvanostatic cycling of cell 632-45-16. Cathode composition was 84 w/o $V_2O_5$ (90 m/o:10 m/o):8 w/o carbon:8 w/o Teflon. Electrolyte was 1.0M $LiClO_4$ in PC.

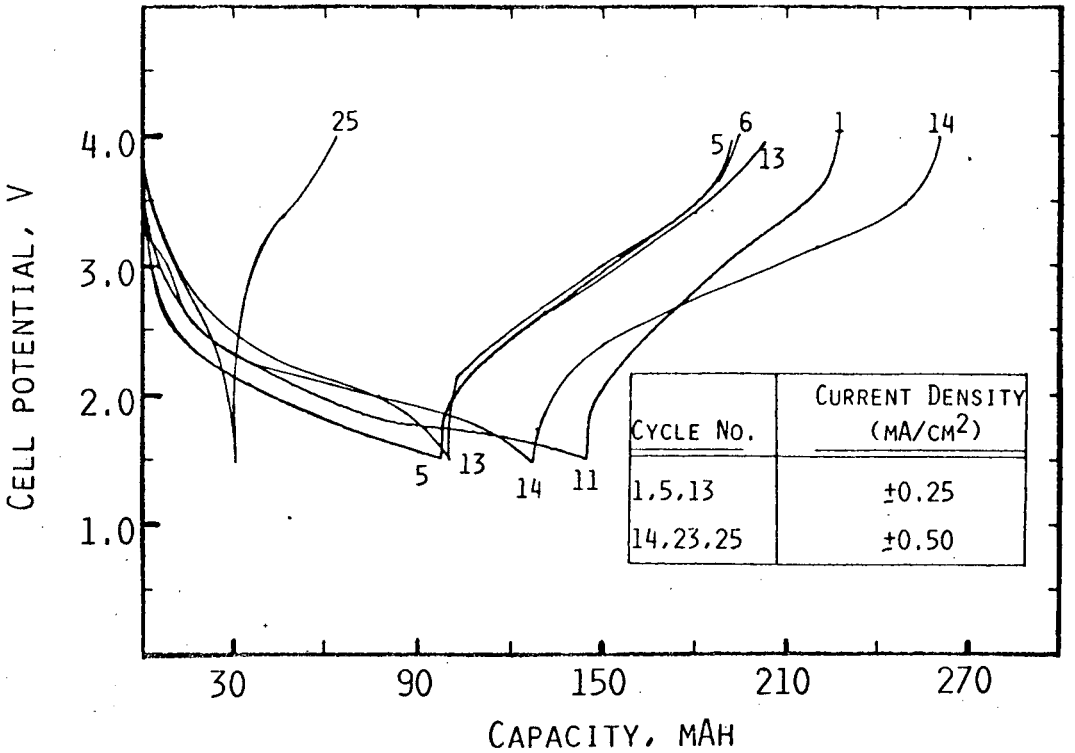


Fig. 13a. Room temperature galvanostatic cycling of cell 627-84-17. Cathode composition was 60 w/o $V_2O_5$-$P_2O_5$ (90 m/o:10 m/o):27 w/o Carbon:13 w/o Teflon. Electrolyte was 1.0M $LiClO_4$ in PC.

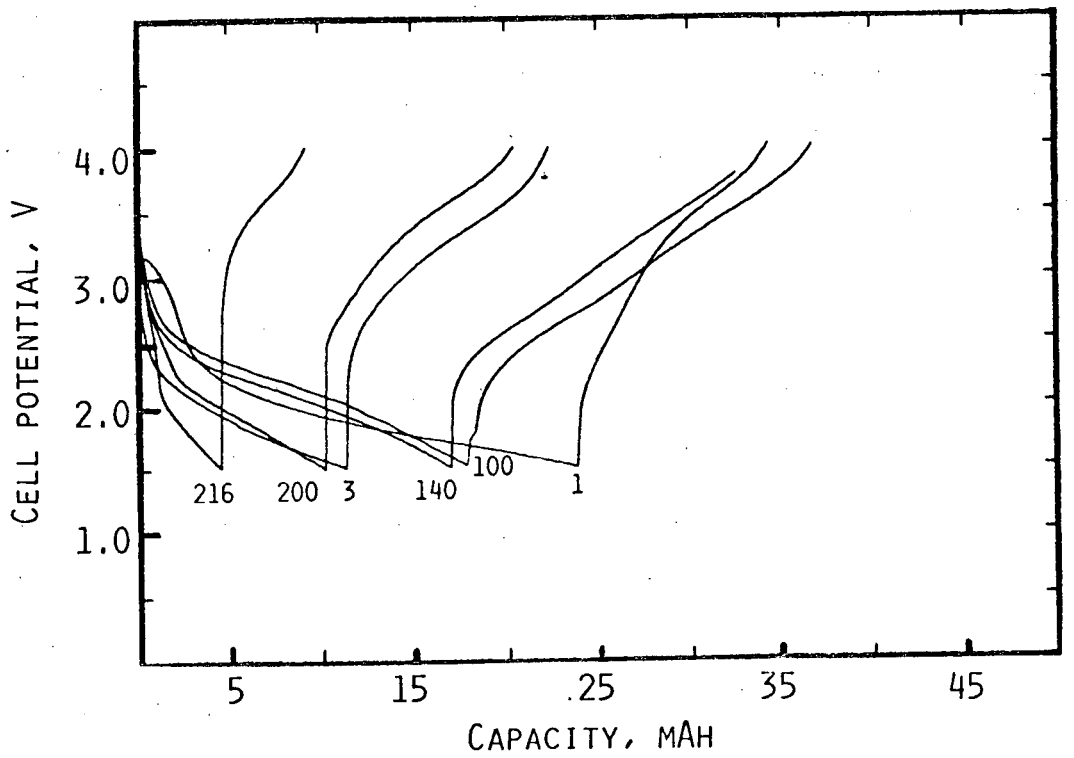


Fig. 13b. Room temperature galvanostatic cycling of cell 660-48-29. Cathode composition was 60 w/o $V_2O_5$-$P_2O_5$ (90 m/o:10 m/o):27 w/o Carbon:13 w/o Teflon. Electrolyte was 1.0M $LiClO_4$ in PC. Current density was ±0.5 mA/cm$^2$ for each cycle.

tribution of particle sizes would have cycled Li better, but this was not the case. Whereas the initial cycles were performed at $\pm 0.5$ mA/cm$^2$, the initial utilization was 1.74 Li/$V_2O_5$ for cell 627-84-17, and only 0.95 Li/$V_2O_5$ for cell 660-48-29. The recharge efficiency of the first cycle was 44% and 54%, respectively, for the sieved and unsieved material. Subsequent recharge efficiencies were 90% or greater, with most being about 100% for both cells. The poor performance by the cell containing the sieved material was especially disconcerting since the cathode thickness was 13 mil, approximately a third of the thickness of the cathode made with the unsieved material. Insufficient compression of the electrode package in this cell was probably responsible for the lack of improvement in rate capability and Li utilization.

The cycling data as a whole shows that the maximum reversible Li utilization of the 90 m/o $V_2O_5$ glass is $\sim$1.6 to 1.7 Li/$V_2O_5$, and that even with carbon loadings as high as 30 w/o, practical current densities greater than 0.5 mA/cm$^2$ are apparently difficult. All of the cycles shown in Figures 11 through 13 exhibit large voltage swings upon switching from discharge to charge.

**$Cr_3O_8$:** A comparison of the X-ray data for $Cr_3O_8$ made at EIC Laboratories with the data from the literature show the material to be single-phase. Four-probe conductivity measurements indicated it to be an insulator, a result in agreement with information reported elsewhere (13,15).

Previously, the greatest degree of Li insertion obtained electrochemically with this material was 4.5 Li/$Cr_3O_8$ (1.5 Li/Cr) in a cell using a cathode of amorphous (high surface area) $Cr_3O_8$ prepared by an autoclave technique. We achieved the same degree of utilization with $Cr_3O_8$ prepared by careful decomposition of $CrO_3$ in air at ambient pressure. The cathode

composition in the cells used for testing this material was 60 w/o $Cr_3O_8$:27 w/o Carbon:13 w/o Teflon. The Li utilization was 4.40 and 3.17 Li/$Cr_3O_8$ for the first discharge and charge, respectively, of a cell cycled by the potential stepping technique. Similarly, a cell cycled first under galvanostatic control yielded 4.49 and 3.39 Li/$Cr_3O_8$ for discharge and charge, respectively, at current densities of 0.25 mA/cm$^2$ for discharge, and 0.13 mA/cm$^2$ for charge.

Figure 14 shows the potentiodynamic cycle obtained with cell 627-97-25. The plateau in the discharge curve at ∿2.9V vs. $Li^+$/Li and the large voltage swing from 1.9 to 2.5V during the subsequent charge are reminiscent of the results reported by Takeda et al. (16). Galvanostatic cycles attempted with this cell at rates from 0.5 to 0.05 mA/cm$^2$ were unsuccessful.

Cell 627-97-24 was cycled galvanostatically, and the resulting curves are shown in Figure 15. As noted above, the Li utilization was 4.49 Li/$Cr_3O_8$ for the first discharge, and 3.39 Li for the first charge. The second discharge capacity was about 60% of the first, and the utilization was 2.71 Li. During the following charge, a cycler malfunction caused the 4.0V charge limit to be exceeded by 0.5V. The charge to 4.0V corresponded to a utilization of 3.09 Li/$Cr_3O_8$. The excess charge capacity was 41 mAh, with an 18 mAh plateau at ∿4.55V probably indicative of some oxidative degradation of the electrolyte solution. This electrolyte reaction may not have had much effect upon the cell's cycle life, since the laboratory test cell configuration ensures that the electrolyte is present in a large excess. The fact that only a small fraction of capacity of the second charge was related to electrolyte decomposition reactions is supported by the fact that the utilization for the third discharge was increased to 3.06 Li/$Cr_3O_8$. During the seventh

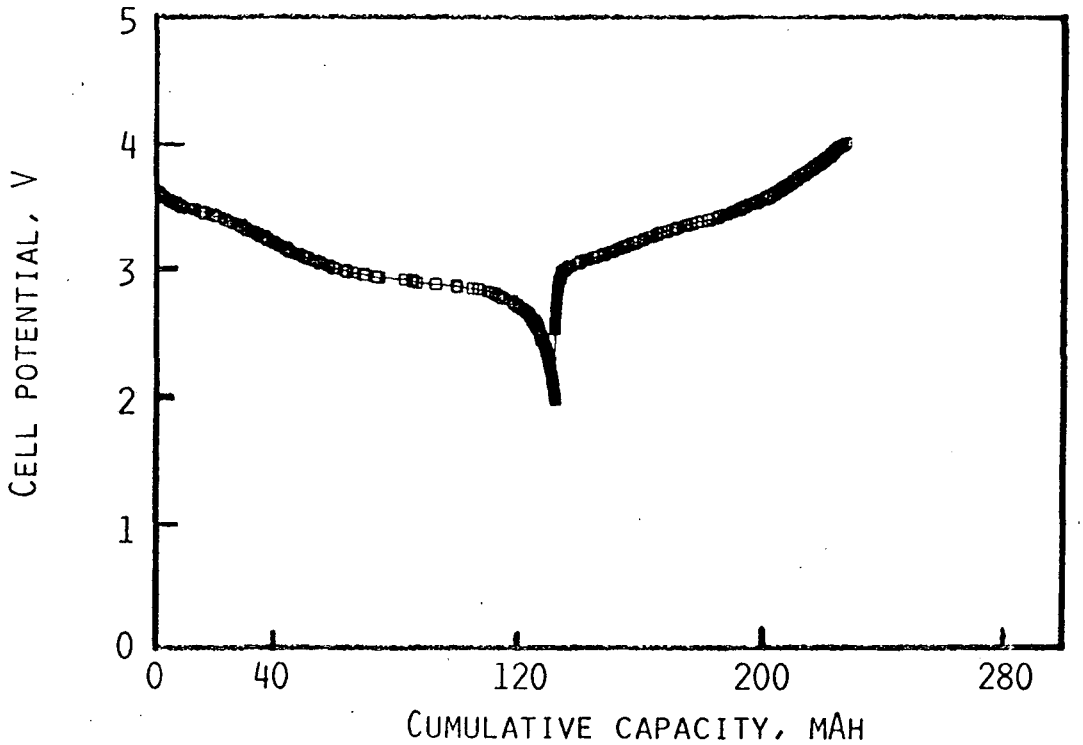


Fig. 14. Potentiodynamic cycling of cell 627-97-25. Cathode composition was 60 w/o $Cr_3O_8$:27 w/o Carbon:13 w/o Teflon. Theoretical cathode capacity was 135 mAh.

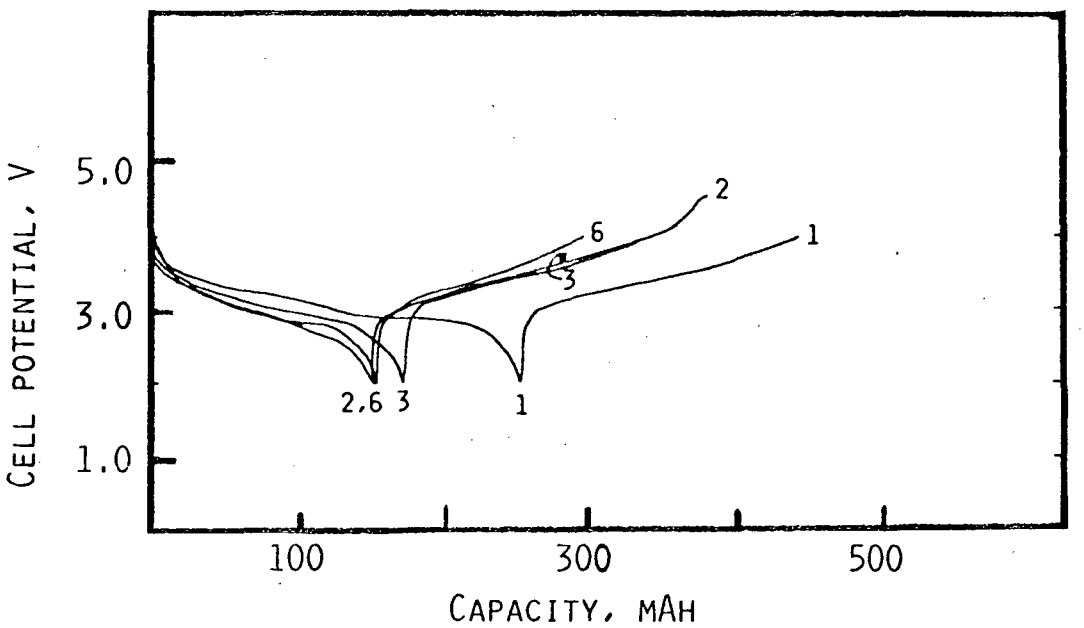


Fig. 15. Galvanostatic cycles for cell 627-97-24. Cathode composition was 60 w/o $Cr_3O_8$:27 w/o Carbon:17 w/o Teflon. Theoretical cathode capacity was 252 mAh. Current density was 0.25 mA/cm$^2$ for discharge and 0.13 for charge.

cycle the discharge rate was increased to 0.5 $mA/cm^2$, but the cell failed because of an internal short.

Insufficient compression of the electrode package in cell 627-97-25 is the probable cause of that cell not cycling under galvanostatic conditions even at rates as low as 0.05 $mA/cm^2$. The data do show, however, that in PC/1.0M $LiClO_4$, $Cr_3O_8$ is a very low rate cathode material.

**$LiCoO_2$:** Cathodes were prepared using samples of $LiCoO_2$ either prepared at EIC Laboratories or purchased from Alfa Chemicals, Inc. Debye-Scherrer X-ray photographs showed the material, regardless of source, to be pure and single-phase. A conductivity of $1.78 \times 10^{-4}$ $(ohm\text{-}cm)^{-1}$ was measured for a pellet prepared from this compound.

Figure 16 is a composite showing the first two potentiodynamic cycles of cell 627-68-10. This cell contained a cathode with the composition 84 w/o $LiCoO_2$:8 w/o Carbon:8 w/o Teflon. As with the other cells, the counter and reference electrodes were Li, and the electrolyte was 1.0M $LiClO_4$ in PC. The theoretical capacity of the cathode was 168 mAh. A total of 39.5 mAh of Li was removed when the potential was stepped from the OCV of 3.34V to 4.0V vs. $Li^+/Li$. The subsequent discharge to 3.4V was 95% efficient, with 37.5 mAh of Li inserted into the cathode. It was found during the second cycle that more Li could be removed by increasing the charge limit to 4.5V. For the cycle obtained under these conditions, 88.3 mAh capacity was observed for the charge, and 76.4 mAh (i.e., 87% of the charge) were observed for the discharge. The danger of using such a high upper voltage limit is the possibility of accelerated electrolyte degradation. A certain amount of electrolyte decomposition may be responsible for the cycling efficiency dropping to 87%. When the cell was switched over to a galvanostatic cycling regime, it was observed that the OCV was 1.30V, probably due to a momentary mechanical

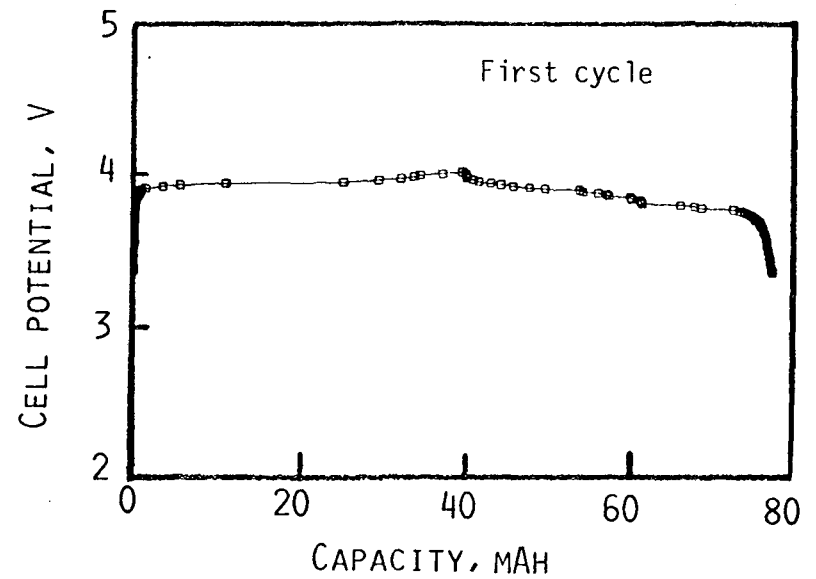


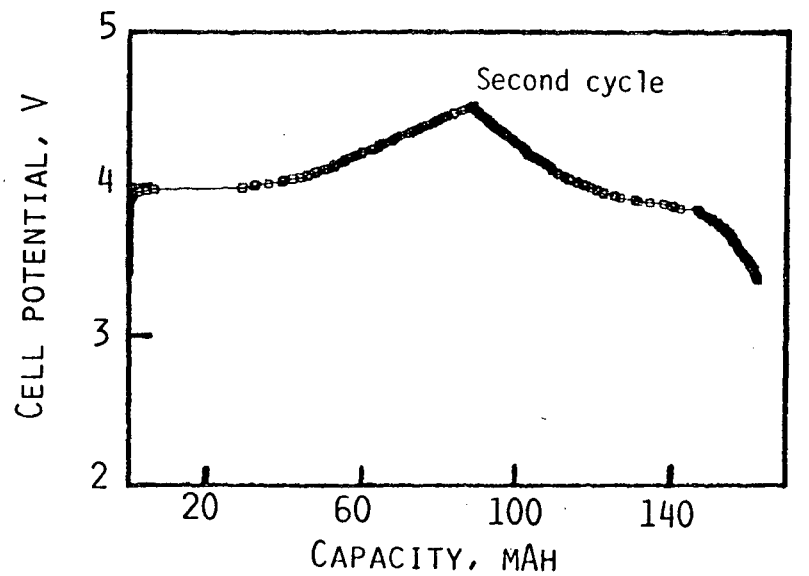


Fig. 16. Potentiodynamic cycling of cell 627-68-10. Cathode composition was 84 w/o $LiCoO_2$:8 w/o Carbon:8 w/o Teflon. Theoretical cathode capacity was 168 mAh.

short. Subsequent charge at 5.0 mA (0.5 mA/cm$^2$) had a capacity of 80 mAh, 2.6 mAh less than the previous potential step discharge, curve a in Figure 17. As shown in Figure 17, only 29 mAh were obtained from the first galvanostatic discharge, and the capacity rapidly decreased with continued cycling. When this cell was disassembled, it was found that the electrical connection to the $LiCoO_2$ electrode was not up to our usual standard, and the electrode itself had not maintained a high degree of integrity, having a rough, uneven surface.

An experiment was performed using a cell that contained $LiCoO_2$ obtained commercially. The cell identification number was 660-50-30, and the cathode composition was 60 w/o $LiCoO_2$:30 w/o Carbon:10 w/o Teflon, with a theoretical capacity of 49 mAh. Due to a mechanical problem which occurred during the cell setup, the OCV dropped from 3.10V to 2.50V. When the cell was potentiodynamically cycled between the voltage limits of 2.5 and 4.5V vs. $Li^+/Li$ (see Fig. 18), it was observed that the cumulative charge capacity to 3.1V was only 0.03 mAh. Total charge capacity to 4.5V was 31.3 mAh, corresponding to 63.9% of the theoretical Li capacity in $LiCoO_2$. Of this capacity, 16.2 mAh were obtained between 2.5 and 4.0V, with the rest observed between 4.0 and 4.5V. Upon discharge, 25.9 mAh were obtained, with only 1.7 mAh between 3.1 and 2.5V. The discharge/charge cycling efficiency was 76%. Subsequently, this cell was cycled galvanostatically at 0.25 mA/cm$^2$, with 23.8 mAh obtained on the first such charge (Curve A, Fig. 19). The discharge capacity decreased rapidly with continued cycling. As Figure 19 shows, by the fourth full galvanostatic cycle, the discharge capacity was 11.4 mAh.

Initially, our interest in using $LiCoO_2$ from another source was based on our observation that cells of the configuration $Li/PC\text{-}LiClO_4/LiCoO_2$ prepared using cathode material synthesized by us appeared to have a much

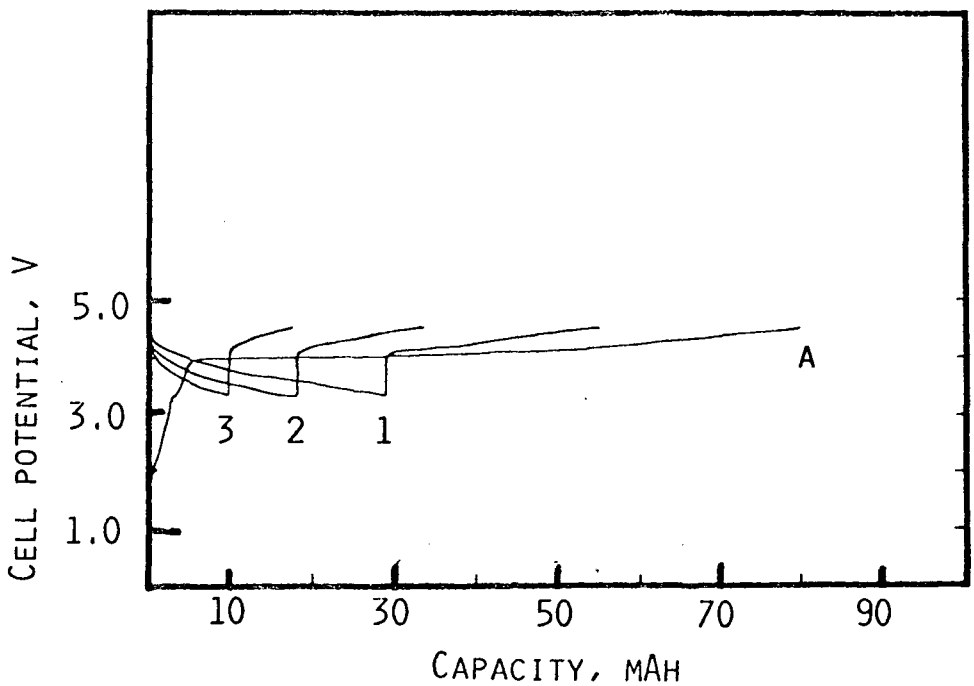


Fig. 17. Galvanostatic cycling curves for cell 627-68-10. Cathode composition was 84 w/o $LiCoO_2$:8 w/o Carbon:8 w/o Teflon. Theoretical cathode capacity was 168 mAh. Current density was $\pm 0.5$ mA/cm$^2$.

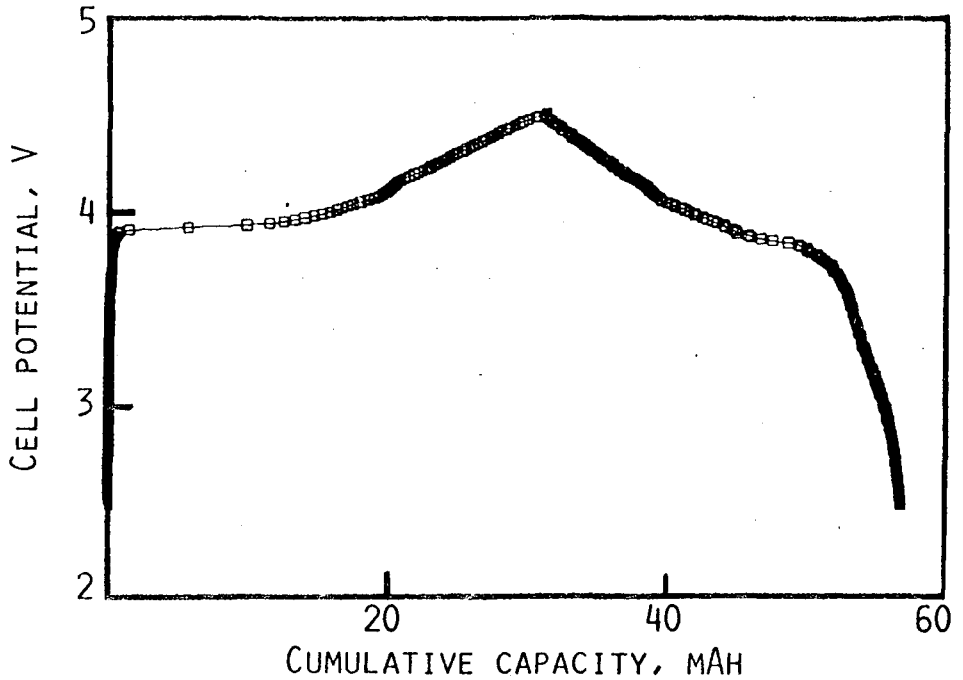


Fig. 18. Potentiodynamic cycle for cell 660-50-30. Cathode composition was 60 w/o $LiCoO_2$:27 w/o Carbon:13 w/o Teflon. Theoretical cathode capacity was 49 mAh.

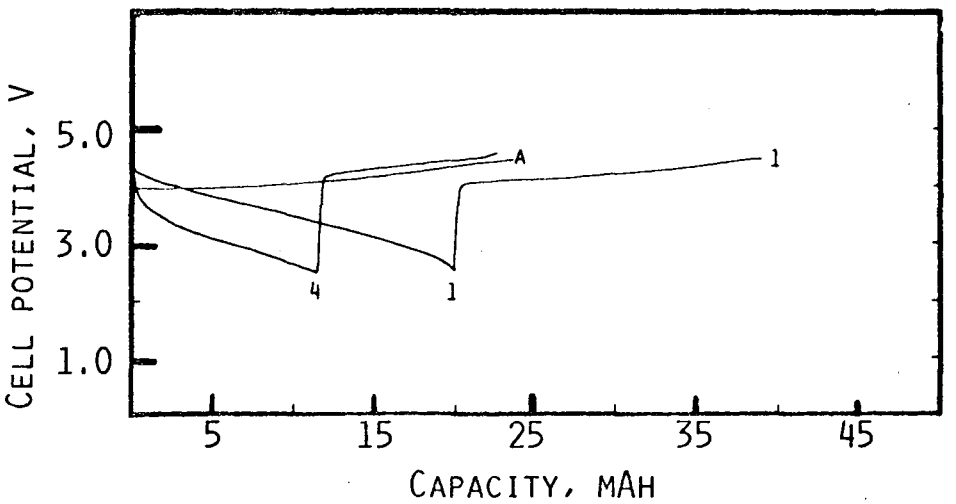


Fig. 19. Galvanostatic cycles for cell 660-50-30. Cathode composition was 60 w/o $LiCoO_2$:27 w/o Carbon:13 w/o Teflon. Current density was 0.25 $mA/cm^2$.

lower OCV than that found in cells prepared by others (14). For cells containing our material, the OCV was typically 3.10 to 3.36V vs. $Li^+/Li$, varying slightly with the particular batch. The Alfa material resulted in an OCV of 3.10V. The fully lithiated material (i.e., $LiCoO_2$) had been reported to result in an OCV of ~3.9V (14). The discrepancy may be due to the fact that for the cell in ref. 14, the voltage was recorded vs. a $Li_{0.1}V_2O_5$ reference electrode, then corrected and reported vs. Li.

### 3.3 Summary

From the data discussed above, it appears that both the vanadium glass and $Cr_3O_8$, with improved cell fabrication technique, might lend themselves to use in low-rate rechargeable Li secondary batteries. The degree of Li utilization and the discharge rates realized in our cells were similar to those previously reported for both compounds. It does not appear that either of these materials is particularly suitable for use in high rate batteries.

Cells containing $LiCoO_2$, regardless of origin or analyzed purity, functioned at current densities far less than the 10 $mA/cm^2$ maximum reported for this compound by Plichta et al. (17). It should be noted that this high rate was obtained previously with cells using methyl acetate as the electrolyte solvent whereas propylene carbonate was used exclusively in our work. A decision on the suitability of this material for use in a rechargeable Li battery should be reserved until the relationship between fabrication technique, solvent, and cell performance (i.e., rate and cycle life) is more thoroughly assessed.

## 4.0 CONCLUSIONS

A convenient procedure for the synthesis of alternative anode materials such as $Li_xFe_2O_3$, $Li_xWO_2$ and LiAl has been developed. The electrochemical behavior of these anodes was studied in cells utilizing a $TiS_2$ cathode and PC-$LiClO_4$ electrolyte. While the lithiated oxides exhibited good reversibility, their equivalent weights are two high for use in high energy density batteries. The experimentally determined value for the reversible Li capacity of $Li_xWO_2$ indicated an equivalent weight of 370 for this anode. The corresponding value for $Li_6Fe_2O_3$ was 201. The results obtained with the β-LiAl, synthesized by the new procedure, were too limited to draw meaningful conclusions regarding its usefulness in practical cells.

Amorphous $V_2O_5$, $Cr_3O_8$ and $Li_xCoO_2$ were evaluated as cathodes for possible use in conjunction with the alternative anodes. While the capacities of a-$V_2O_5$ and $Cr_3O_8$ are attractive for practical applications, these positive electrodes exhibited rather low rate capabilities. The performance of $Li_xCoO_2$ was inferior to the results previously reported for this cathode and might have been influenced by the electrolyte employed in our studies.

## 5.0 REFERENCES


1. K. M. Abraham, J. Power Sources, 14, 179 (1985).

2. D. T. Fouchard, Proceedings of the 32nd Power Sources Symposium, Cherry Hill, NJ, 1986, p. 218.

3. K. M. Abraham and S. B. Brummer, Chapter 14 in "Lithium Batteries", J. P. Gabano, Editor, Academic Press, New York, 1983.

4. M. Lazzari and B. Scrosati, J. Electrochem. Soc., 127, 773 (1980).

5. B. DiPietro, M. Patriarca and B. Scrosati, J. Power Sources, 8, 289 (1982).

6. T. O. Brun, J. D. Jorgensen, M. Misawa, F. J. Rotella and S. Susman, J. Electrochem. Soc., 129, 2509 (1982).

7. Y. Geronov, P. Zlatilova and G. Staikov, J. Power Sources, 12, 155 (1984).

8. K. M. Abraham, D. M. Pasquariello and F. J. Martin, J. Electrochem. Soc., 133, 643 (1986).

9. R. D. Rieke and P. M. Hudnall, J. Am. Chem. Soc., 94, 7178 (1972).

10. M. B. Dines, Mat. Res. Bull., 10, 284 (1975).

11. J. J. Auborn and Y. L. Barberio, J. Electrochem. Soc., 134, 638 (1987).

12. Y. Sakurai and J. Yamaki, J. Electrochem. Soc., 132, 512 (1985).

13. J. O. Besenhard and R. Schollhorn, J. Electrochem. Soc., 124, 968 (1977).

14. K. Mizushima, P. C. Jones, P. J. Wiseman and J. B. Goodenough, Mat. Res. Bull. 15, 783 (1980).

15. J. O. Besenhard, J. Heydecke, E. Wudy and H. P. Fritz, Solid State Ionics, 8, 61 (1983).

16. Y. Takeda, R. Kanno, Y. Tsuji and O. Yamamoto, J. Electrochem. Soc., 131, 2006 (1984).

17. E. Plichta, S. Slane, M. Nichiyama and M. Salomon, The Spring Meeting of the Electrochemical Society, Philadelphia, PA, 1987, Abstract No. 546.

*LAWRENCE BERKELEY LABORATORY*
*TECHNICAL INFORMATION DEPARTMENT*
*UNIVERSITY OF CALIFORNIA*
*BERKELEY, CALIFORNIA 94720*